Excited State Processes in Ruthenium(II)/Pyrenyl Complexes Displaying Extended Lifetimes

Daniel S. Tyson, Kevin B. Henbest,† Jason Bialecki, and Felix N. Castellano*

Department of Chemistry and Center for Photochemical Sciences, Bowling Green State University, Bowling Green, Ohio 43403

Received: May 9, 2001; In Final Form: June 25, 2001

The synthesis and photophysical properties of two Ru(II) diimine complexes bearing one (dyad) and three (tetrad) pyrenyl units, respectively, are presented. The pyrene chromophore in each metal complex is tethered through a single C−C bond in the 5-position of 1,10-phenanthroline (py-phen). Both Ru(II) complexes display increased absorption cross sections near 340 nm largely due to the presence of the pyrenyl chromophore(s). Excitation from 300 to 540 nm results exclusively in the observation of metal-to-ligand charge transfer (MLCT) based emission that is exceptionally long lived, 23.7 μs and 148 μs in deaerated CH_3CN, respectively. This luminescence was analyzed using steady-state and time-resolved techniques at room temperature and 77 K. The tetrad complex, $[Ru(py\text{-}phen)_3]^{2+}$, displays a dynamic self-quenching reaction at room temperature in dilute CH_3CN solutions that is well modeled by a Stern−Volmer expression. The excited-state processes occurring between the MLCT core and the pyrenyl units were further evaluated with ultrafast transient absorption spectroscopy and conventional flash photolysis. Formation of the ^{3}pyrene absorption was directly monitored in both complexes and ranged from 2.8×10^{10} s^{-1} in $[Ru(bpy)_2(py\text{-}phen)]^{2+}$ to 2.4×10^{11} s^{-1} in $[Ru(py\text{-}phen)_3]^{2+}$. In both cases, the transient absorption spectra contain features of ^{3}pyrene excited states, whereas the room-temperature luminescence is MLCT-based, both decaying with the same kinetics. This is consistent with the formation of a thermal excited-state equilibrium between the two triplet states at room temperature. Both Ru(II) complexes were found to sensitize the production of molecular singlet oxygen with a quantum efficiency of 0.69, measured by observing the characteristic $^1O_2$ luminescence at 1270 nm.

Introduction

Luminescence probes that display long decay times are becoming increasingly important in biophysics, high-throughput screening, clinical chemistry, and lifetime-based chemical sensing.[1−4] Transition metal complexes displaying metal-to-ligand charge transfer (MLCT) excited states[5] have shown promise in such luminescence-based technologies.[1−4] In the interest of expanding these initial efforts, new MLCT compounds with prolonged emission decay times warrant further investigation.

There has been recent interest in the study of bichromophores consisting of a Ru(II) diimine complex that displays MLCT excited states covalently linked to pyrene using a variety of tethers.[6−11] In all cases the excited state lifetimes observed from these complexes were significantly enhanced relative to model compounds. The focus of much of this work has been in measuring the various kinetic processes involved and in classifying the mechanism(s) responsible for the lifetime extension. All systems to date possess lifetimes that are modulated by the relative triplet energy levels of the Ru(II) and pyrene units, the nature of the bridging group connecting them, and the molecular orientation between the fragments. In the cases where the Ru(II) and pyrenyl chromophores establish a thermal triplet equilibrium,[6−10] we have suggested that the equilibrium process can be systematically controlled by adding additional pyrene molecules to the ligand periphery.[10] This favors the formation of "pyrene-like" triplets in the equilibrium mixture, further extending the lifetime of the complex. In addition to these interesting triplet−triplet processes, it has also been shown that singlet−singlet energy transfer between the pyrenyl moiety and the Ru(II) core is also efficient,[7,10] where the pyrenyl units provide a UV light-harvesting antenna system for the sensitization of MLCT-based emission.

We have successfully prepared two new Ru(II)/pyrene complexes, $[Ru(bpy)_2(py\text{-}phen)]^{2+}$ and $[Ru(py\text{-}phen)_3]^{2+}$, where bpy is 2,2′-bypyridine and py-phen is 5-pyrenyl-1,10-phenanthroline. Both complexes display enhanced excited-state lifetimes at room temperature in deaerated CH_3CN, 23.7 and 148 μs, respectively. These extended lifetimes are described by an excited-state equilibrium between the triplet states of the pyrene unit(s) and the core Ru(II) complex. In the present study, the pyrene chromophore(s) can play a dual role as both energy transfer donor and acceptor. A preliminary report on the notably long excited-state lifetime exhibited by $[Ru(py\text{-}phen)_3]^{2+}$ has recently appeared.[12]

Experimental Section

General. All synthetic manipulations were performed under an inert and dry argon atmosphere using standard techniques. Anhydrous THF, anhydrous ether, 2,2′-bipyridine (bpy), 1,10-phenanthroline (phen), *n*-butyllithium (1.6 M in hexanes), $Pd(PPh_3)_4$, barium hydroxide, and triisopropyl borate were obtained from Aldrich and used as received. All other reagents and materials from commercial sources were used as received. $Ru(bpy)_2Cl_2$[13] and $Ru(DMSO)_4Cl_2$[14] were prepared according to published procedures.

* Corresponding author. E-mail: castell@bgnet.bgsu.edu. Fax: (419) 372−9809.

† Present Address: Oxford University, Physical and Theoretical Chemistry Laboratory, South Parks Road, Oxford, U.K.

10.1021/jp011770f CCC: $20.00
Published on Web 08/02/2001

^{1}H NMR spectra were recorded on a Varian Gemini 200 (200 MHz) spectrometer. All chemical shifts are referenced to residual solvent signals previously referenced to TMS. GC and DIP mass spectra were measured in-house using a Shimadzu QP5050A spectrometer. FAB mass spectra were measured at the University of Maryland College Park Mass Spectrometry Laboratory. Elemental analyses were obtained at the Analytical Facilities, University of Toledo.

Syntheses. *5-Bromo-1,10-phenanthroline.* This compound was prepared according to a published procedure.[15] ^{1}H NMR ($CDCl_3$): δ 9.23 (q, 2H), 8.69 (dd, 1H), 8.20 (dd, 1H), 8.17 (s,1H), 7.72 (dq, 2H). MS (GC): *m*/*z* 258/260 M^+.

3-Bromopyrene. This compound was prepared as described in the literature.[16] mp 93.5−95.5 °C (Lit. 94.5−95.5 °C). ^{1}H NMR (d_6-acetone): δ 8.46−8.31 (br m, 5H), 8.27−8.09 (br m, 4H). MS (DIP): *m*/*z* 280/282 M^+.

3-Pyreneboronic Acid. 3-Bromopyrene (2.00 g, 7.12 mmol) was dissolved in a mixture of dry THF (150 mL) and dry ether (150 mL). The pale yellow solution was cooled to −78 °C under argon. *n*-Butyllithium (4.9 mL, 7.83 mmol) was added dropwise with stirring to produce a bright yellow solution, which slowly became cloudy. The mixture was held at −78 °C for 10 min, at −10 °C for 10 min, then at −78 °C for 30 min. Triisopropyl borate (4.93 mL, 21.36 mmol) was then added dropwise. The reaction was held at −78 °C for 30 min and slowly became yellow-orange and clear. This solution was warmed to 0 °C over 3 h, during which time it became cloudy yellow. The mixture was slowly brought to ambient temperature and maintained at room temperature for 1.5 days. Water (100 mL) was added to the reaction vessel and the mixture stirred vigorously for 1 h. The aqueous layer was extracted with ether (2 × 25 mL) and the combined organic layers were washed with water (2 × 50 mL), dried over $MgSO_4$, filtered, and rotary evaporated to dryness to yield the solid product, which was used without further purification (1.43 g, 82% yield). ^{1}H NMR ($CDCl_3$): δ 8.30−8.17 (br m, 4H), 8.14−7.98 (br m, 5H), OH protons not resolved. MS (DIP): *m*/*z* 246 M^+.

5-Pyrenyl-1,10-phenanthroline (py-phen). 5-Bromo-1,10-phenanthroline (191 mg, 0.74 mmol) and 3-pyrene boronic acid (200 mg, 0.81 mmol) were dissolved in 30 mL toluene and 10 mL ethanol. The yellow solution was degassed with Ar for 30 min. A saturated aqueous solution of $Ba(OH)_2$ (40 mL) was added, and the biphasic mixture was degassed an additional 30 min. $Pd(PPh_3)_4$ (34.7 mg, 0.03 mmol) was added and the reaction mixture refluxed with vigorous stirring under Ar for 2 days. Once cool, the layers were separated and the aqueous layer was extracted with toluene (3 × 10 mL) and the combined organic extracts were washed with water (3 × 20 mL). The organic fractions were dried over $MgSO_4$, filtered, and rotary evaporated to a brown oily residue. The oil was triturated with chloroform, petroleum ether added, and the mixture was chilled to promote further crystallization. The light yellow product was collected as a solid by vacuum filtration on a Buchner funnel (194 mg, 63% yield). This solid decomposed above 245 °C. Anal. Calcd for $C_{28}H_{16}N_2$: C, 88.39; H, 4.23; N, 7.36. Found: C, 86.56; H, 4.18; N, 6.76. ^{1}H NMR (d_6-acetone): δ 9.21 (dd, 1H), 9.13 (dd, 1H), 8.53 (dd, 1H), 8.47 (d, 1H), 8−8.4 (br m, 8H), 7.82 (q, 1H), 7.75 (dd, 1H), 7.68 (d, 1H), 7.54 (q, 1H). MS (DIP): *m*/*z* 380 M^+.

Bis(2,2′-bypyridine)(5-pyrenyl-1,10-phenanthroline)ruthenium-(II) hexafluorophosphate, [Ru(bpy)$_2$(py-phen)](PF$_6$)$_2$. $Ru(bpy)_2Cl_2 \cdot 2H_2O$ (49.4 mg, 0.095 mmol) and 5-pyrenyl-1,10-phenanthroline (39.9 mg, 0.105 mmol) were suspended in methanol (40 mL), protected from light, and refluxed for 3 h while stirring under Ar. The reaction solution was cooled to room temperature, filtered, and water (10 mL) was added to the filtrate. Dropwise addition of 20 mL saturated NH_4PF_6(aq) generated a bright orange precipitate. The precipitate was collected by vacuum filtration through a fine glass frit and washed with water, followed by diethyl ether to afford the crude orange product. The complex was purified by column chromatography on Sephadex LH-20 (25 × 2 cm, MeOH) and precipitated by the addition of concentrated NH_4PF_6 (aq) (52 mg, 52% yield). Anal. Calcd for $C_{48}H_{32}N_6RuP_2F_{12} \cdot 2H_2O$: C, 51.48; H, 3.24; N, 7.50. Found: C, 51.24; H, 3.93; N, 7.49. MS (FAB): *m*/*z* 938.9 [M − PF_6]$^+$, 794.1 [M − 2PF_6]$^{2+}$.

Tris(5-pyrenyl-1,10-phenanthroline)ruthenium(II) hexafluorophosphate, [Ru(py-phen)$_3$](PF$_6$)$_2$. $Ru(DMSO)_4Cl_2$ (33.8 mg, 0.070 mmol) and 5-pyrenyl-1,10-phenanthroline (87.4 mg, 0.230 mmol) were dissolved in 95% ethanol (10 mL), protected from light, and refluxed for 24 h under Ar. This solution was cooled to room temperature, 5 mL H_2O was added, and the mixture was filtered. Excess NH_4PF_6(aq) was added and a dark orange solid immediately precipitated. The solid was filtered through a fine glass frit and washed with water followed by ether to afford the crude product. The complex was purified by column chromatography on Sephadex LH-20 (25 × 2 cm, MeOH) and precipitated by the addition of concentrated NH_4PF_6(aq) (45 mg, 46% yield). Anal. Calcd for $C_{84}H_{48}N_6RuP_2F_{12} \cdot 6H_2O$: C, 62.33; H, 3.60; N, 5.01. Found: C, 61.54; H, 3.13; N, 5.09. MS (FAB): *m*/*z* 1387.4 [M − PF_6]$^+$, 1242.4 [M − 2PF_6]$^{2+}$.

Physical Measurements. Absorption spectra were measured with a Hewlett-Packard 8453 diode array spectrophotometer, accurate to ±2 nm. Static luminescence spectra were obtained with a single photon counting spectrofluorimeter from Edinburgh Analytical Instruments (FL/FS 900). The temperature in the fluorimeter was maintained at 22 ± 1 °C for all measurements with a Neslab RTE−111 circulating bath. Excitation spectra were corrected with a photodiode mounted inside the fluorimeter that continuously measures the Xe lamp output. Frozen glass emission samples at 77 K were prepared by inserting a 5 mm (internal diameter) NMR tube containing a 10^{-5} M solution (butyronitrile or 4:1 EtOH/MeOH) of the appropriate complex into a quartz-tipped finger dewar of liquid nitrogen. Luminescence quantum yields were referenced to $[Ru(bpy)_3]^{2+}$ in CH_3CN ($\Phi_r = 0.062$), as described previously.[10] All luminescence experiments used optically dilute solutions (OD = 0.09−0.11) prepared in spectroscopic grade CH_3CN unless otherwise stated. All luminescence samples in 1 cm^2 anaerobic quartz cells (Starna Cells) were deoxygenated with solvent-saturated argon for at least 30 min prior to measurement.

Emission lifetimes were measured with an apparatus described previously,[10] using a nitrogen-pumped broadband dye laser (PTI GL-3300 N_2 laser, PTI GL-301 dye laser, Coumarin 460 or Coumarin 500) as the excitation source. Pulse energies were typically attenuated to ∼100 μJ/pulse, measured with a Molectron joulemeter (J4−05). An average of 128 transients were collected, transferred to a computer, and processed using Origin 6.0.

Nanosecond time-resolved absorption spectroscopy was performed using instrumentation that has been described previously.[10] The excitation source was the unfocused second harmonic (532 nm, 7 ns fwhm) output of a Nd:YAG laser (Continuum Surelite I). Typical excitation energies were 2−3 mJ/pulse. Samples were continuously purged with a stream of high purity argon or nitrogen gas throughout the experiments. The data, consisting of a 10-shot average of both the signal and the baseline, were analyzed with programs of local origin.

TABLE 1: Spectroscopic and Photophysical Data

complex	λ_{max}, nm (ϵ, M^{-1} cm^{-1})	$\lambda_{em\ max}$, nm (298 K)	$\lambda_{em\ max}$, nm (77 K)	τ_{PL},[a] μs (298 K)	τ_{T-Tabs},[b] μs	τ, ms (other components) (77 K)	Φ_r[c]
$[Ru(bpy)_3]^{2+}$	452 (13,000)	615	580, 628	0.920 ± 0.05	1.02 ± 0.05	5.1 ± 0.25 μs	0.062 ± 0.006
$[Ru(bpy)_2(py\text{-}phen)]^{2+}$	339 (24,200) 451 (13,700)	606	601, 660	23.7 ± 1.2	20.43 ± 2.5	41.6 ± 2.0 (5.2 μs, 10.8 ns)	0.071 ± 0.011
$[Ru(py\text{-}phen)_3]^{2+}$	340 (57,700) 449 (16,000)	597	602, 663	148 ± 8.5	142 ± 12	46.0 ± 2.0 (5.0 μs, 14.8 ns)	0.064 ± 0.01
Py-phen	342 (31,200) 326 (23,900) 312 (12,500)	446	598, 661	6.35 ± 0.05 ns[d]	131 ± 10[e]	4.10 ± 0.5 μs (12.3 ns)	NA

[a] Lifetimes represent an average of at least six measurements and have an uncertainty of less than 10%. Here the data were obtained using 458 ± 2 nm excitation. [b] The lifetime of the triplet−triplet pyrene absorption, measured at 410 nm with 450 nm excitation. [c] Error bars represent reproducibility within 2σ, including the uncertainty in the measurement of the standard. [d] Measured by TCSPC with 343 nm excitation. [e] 355 nm excitation, transient absorption detected at 500 nm.

The laser system for the ultrafast transient absorption spectrometry experiments has been fully described elsewhere.[17] Briefly, the setup included a Ti:sapphire seed laser (Spectra-Physics Tsunami model 3941-MIS) pumped by a diode-pumped 5 W cw Nd:YAG laser (Spectra-Physics Millennia). The Tsunami output (ca. 10 nJ, 70 fs) was steered into a Ti:sapphire regenerative amplifier (Positive Light Spitfire) that was pumped with a frequency-doubled (527 nm), Q-switched Nd:YLF laser (Positive Light Merlin). The output of the amplifier was typically 1 mJ/pulse (fwhm = 100 fs) at a repetition rate of 1 kHz. The angle between the pump and probe beam was maintained at 5°−7°. The sample flow-through cell had an optical path length of 2 mm and was connected to a solution reservoir and flow system. The pump beam was chopped with a mechanical chopper to produce test and reference signals, which were measured with a CCD spectrograph (Ocean Optics, SD2000). Typically, 4000 excitation pulses were averaged to obtain the transient spectrum at a particular delay time. Shutters were used to block the pump and continuum beams to minimize exposure. The instrument response of this spectrometer was determined to be 500 fs. The solutions possessed an absorbance of 0.8 at the excitation wavelength of 400 nm in the 2 mm flow cell. The absorbance spectra of the solutions measured before and after the experiment were the same within experimental error, ensuring sample stability.

Singlet molecular oxygen was detected following 532 nm pulsed laser excitation (Nd:YAG) by observation of its characteristic luminescence at 1270 nm using a silicon-filtered Ge photocell (Applied Detector Corp.) cooled to 77 K with liquid N_2. This experiment is also described in detail elsewhere.[18] Initial yields of singlet oxygen were measured as a function of laser intensity over regions where the characteristic $^1O_2$ emission was directly proportional to the incident photon intensity. This was estimated by signal averaging 256 laser shots at each laser power, where the 1270 nm luminescence signal at $t = 0$ was used to obtain the relative yield of singlet oxygen sensitized by each metal complex in air-equilibrated CH_3CN. These data were directly compared to those obtained with tetraphenylporphyrin (TPP) in air-equilibrated benzene ($\Phi = 0.58$)[19] that had an exactly matched absorbance at 532 nm. The slopes derived from the plots of $^1O_2$ emission intensity vs percent laser energy in each sample were used to calculate the quantum yields for $^1O_2$ sensitization with TPP as a primary standard.

Results and Discussion

The structures of the two Ru(II) complexes in this study are given in Scheme 1. The diimine ligand, py-phen, was synthesized from 5-bromo-1,10-phenanthroline and 3-pyrene-boronic acid using a standard Suzuki coupling. Both Ru(II) complexes were prepared following standard protocols, with final purification achieved by chromatography on Sephadex LH-20. The purity of these complexes was established by FAB mass spectrometry and HPLC.

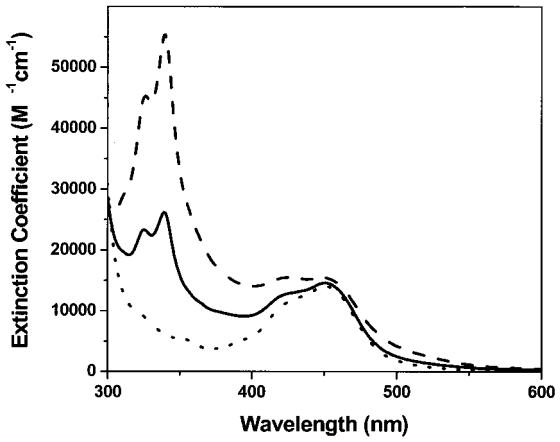

Figure 1. Electronic spectra of $[Ru(bpy)_3]^{2+}$ (dotted line), $[Ru(bpy)_2(py\text{-}phen)]^{2+}$ (solid line), and $[Ru(py\text{-}phen)_3]^{2+}$ (dashed line) in CH_3CN.

SCHEME 1

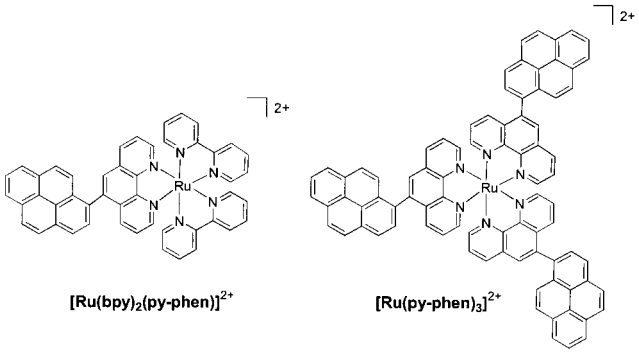

The spectroscopic and photophysical data are presented in Table 1. Figure 1 displays the absorption spectra for $[Ru(bpy)_3]^{2+}$, $[Ru(bpy)_2(py\text{-}phen)]^{2+}$, and $[Ru(py\text{-}phen)_3]^{2+}$ in CH_3CN. Each complex possesses the typical MLCT absorption near 450 nm, while $[Ru(bpy)_2(py\text{-}phen)]^{2+}$ and $[Ru(py\text{-}phen)_3]^{2+}$ have increased absorption near 340 nm that is largely attributed to the pyrenyl chromophores. These spectra represent the sum of the individual chromophoric units with no new features, suggesting that there is no significant electronic interaction between the Ru(II) core and the pyrene molecule(s). This is supported by the molecular modeling of py-phen (MMFF94,

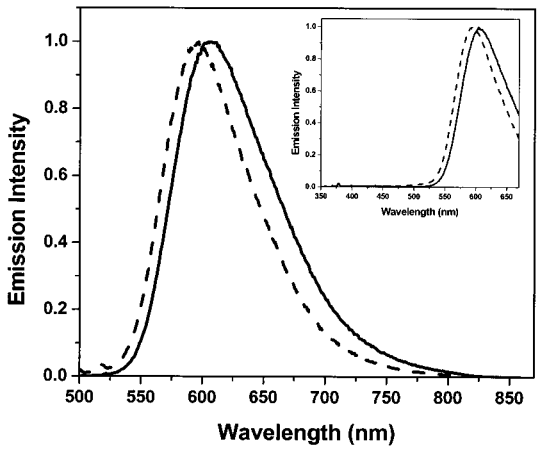

Figure 2. Uncorrected emission spectra of $[Ru(bpy)_2(py\text{-}phen)]^{2+}$ (solid line) and $[Ru(py\text{-}phen)_3]^{2+}$ (dashed line) in CH_3CN at 22 °C using 450 nm excitation. Inset: Uncorrected emission spectra of $[Ru(bpy)_2(py\text{-}phen)]^{2+}$ (solid line) and $[Ru(py\text{-}phen)_3]^{2+}$ (dashed line) in CH_3CN at 22 °C using 340 nm excitation.

Spartan 5.0)[20] which revealed that the minimum energy structure has the pyrene at a 54° tilt relative to the 1,10-phenanthroline portion, greatly disrupting the conjugation between the units. This modeling appears to be justified in the observed UV−vis data. Importantly, good photoselectivity can be achieved due to the wide separation of the pyrene (340 nm) and the MLCT (450 nm) absorption bands. By comparing the molar extinction coefficients of each Ru(II)/pyrene complex with that of the model core complex $[Ru(bpy)_3]^{2+}$, the relative percentage of incident light absorbed by the pyrene moieties can be calculated. In $[Ru(bpy)_2(py\text{-}phen)]^{2+}$, ~67% of the light absorbed at 340 nm is due to pyrene, whereas ~86% of the absorbed energy at 340 nm is captured by the pyrene molecules in $[Ru(py\text{-}phen)_3]^{2+}$. In this respect, the pyrene chromophores serve as UV light-harvesting antennae. The enhanced absorption cross sections in the UV are suitable for efficient light-harvesting in this region.

The photoluminescence spectra of $[Ru(bpy)_2(py\text{-}phen)]^{2+}$ and $[Ru(py\text{-}phen)_3]^{2+}$ ($\lambda_{ex} = 450$ nm) are displayed in Figure 2. In both complexes, the emission band is centered near 600 nm with quantum yields of 0.071 and 0.064, respectively, indicative of MLCT-based luminescence. Direct excitation into the pyrene chromophores (340 nm) results exclusively in MLCT-based emission (Figure 2 inset). The excitation spectra of each complex are nearly superimposable with the corresponding absorption spectra. These observations are consistent with either highly efficient singlet energy transfer or direct intersystem crossing from the pyrenyl antennae to the Ru(II) core. It should be noted that the fluorescence spectrum of py-phen in CH_3CN is markedly different that that displayed by pyrene (Figure 1S), and the excited state lifetime of py-phen is 6.35 ns, which is substantially shorter than pyrene and indicates strong electronic coupling between pyrene and 1,10-phenanthroline. These photophysical observations are consistent with those recently observed in 2,2′-bipyridine compounds tethered to pyrene across a single C−C bond and can be interpreted as excited states possessing some degree of intramolecular charge-transfer character.[21]

Time-resolved emission decays for $[Ru(bpy)_2(py\text{-}phen)]^{2+}$ and $[Ru(py\text{-}phen)_3]^{2+}$ in CH_3CN at 22 °C measured under deaerated conditions are shown in Figure 3. The recovered excited-state lifetimes of 23.8 ± 1.2 μs and 148 ± 8.5 μs for $[Ru(bpy)_2(py\text{-}phen)]^{2+}$ and $[Ru(py\text{-}phen)_3]^{2+}$, respectively, were independent of excitation wavelength (350−532 nm) and could be adequately fit with a single-exponential model.[22] Time-resolved emission spectra obtained for both complexes at room temperature

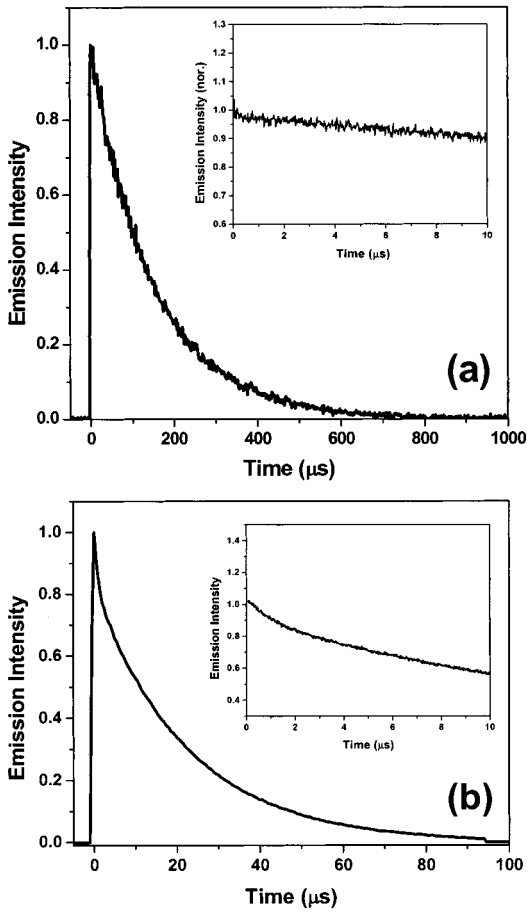

Figure 3. Time-resolved photoluminescence decays of (a) $[Ru(py\text{-}phen)_3]^{2+}$ and (b) $[Ru(bpy)_2(py\text{-}phen)]^{2+}$ in deaerated CH_3CN obtained with 458 nm pulsed excitation and detected at 600 nm. Insets: decay data expanded to include only the first 10 μs.

decayed symmetrically (not shown), consistent with radiative decay from a single excited state. The emission properties of both complexes ($[Ru(py\text{-}phen)_3]^{2+}$ to a greater extent) were considerably sensitive to oxygen and temperature. Consequently, care was taken to thoroughly deaerate each sample while maintaining a restricted temperature range (22 ± 1 °C). The initial time-resolved emission decays of each complex are expanded in Figure 3 as insets. No measurable deviation from single-exponential behavior was observed for $[Ru(py\text{-}phen)_3]^{2+}$ down to our instrument response (15 ns). However, for $[Ru(bpy)_2(py\text{-}phen)]^{2+}$, nonexponential behavior was apparent. In this complex the expanded emission decay could be fit as a sum of two exponentials with components of ~1 μs and 23 μs. Due to the small triplet energy gap (discussed later) between the pyrene and the Ru(II) core, the short luminescence component in $[Ru(bpy)_2(py\text{-}phen)]^{2+}$ could be interpreted in two ways: either as a result of luminescence from an additional (nonequilibrated) excited state or a MLCT excited state that is in a preequilibrium condition.[11,23] Given that the room-temperature time-resolved emission spectra display a single band, it is likely that the short emission component results from the latter.

The transient absorption spectra of $[Ru(bpy)_2(py\text{-}phen)]^{2+}$ and $[Ru(py\text{-}phen)_3]^{2+}$ following a 532 nm laser pulse are presented in Figure 4 along with two model compounds, $[Ru(bpy)_3]^{2+}$ and py-phen. The excited-state spectrum of py-phen was generated with 355 nm laser pulses. The excited-state absorption difference spectra of the dyad and tetrad are strikingly similar to that of py-phen over the measurable time range, indicating

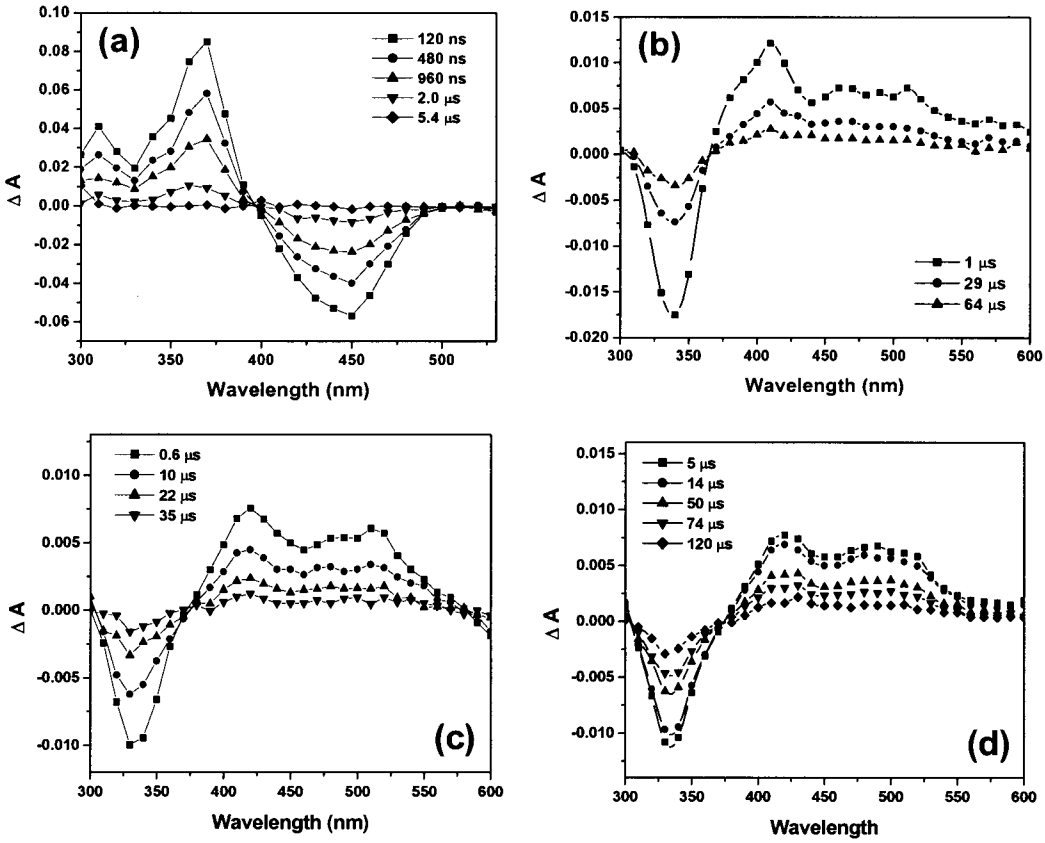

Figure 4. Excited-state absorption difference spectra for (a) $[Ru(bpy)_3]^{2+}$, (b) py-phen, (c) $[Ru(bpy)_2(py\text{-}phen)]^{2+}$, and (d) $[Ru(py\text{-}phen)_3]^{2+}$ in deaerated CH_3CN following 532 nm or 355 nm pulsed excitation.

the presence of pyrene-localized triplet excited states. The question of how these states are formed, either through direct intersystem crossing from the ^{1}MLCT states or through triplet energy transfer from ^{3}MLCT states, will be discussed below. The transient absorption spectra of each complex decays with the same single-exponential kinetics within experimental error as the corresponding luminescence decays. The fact that the ^{3}MLCT and ^{3}pyrene states decay with the same kinetics and clearly coexist demonstrates that the two species are equilibrated in both complexes at room temperature.

In an attempt to directly measure the rate of formation of the pyrene triplet excited states, ultrafast transient absorption spectroscopy was employed. Similar spectral profiles were obtained for both complexes following a 150 fs laser pulse. For brevity, only the transient absorption spectra and kinetic profile for $[Ru(bpy)_2(py\text{-}phen)]^{2+}$ are shown in Figure 5. The absorption transient at 500 nm following a 400 nm laser pulse is assigned to the formation of triplet pyrene. The kinetic fit of the transient growth at 500 nm was single exponential with a rate of 2.8×10^{10} s^{-1} (35.7 ps), consistent with a literature value reported for a related Ru(II)-pyrene dyad.[9] The ultrafast absorption transients of $[Ru(py\text{-}phen)_3]^{2+}$ displayed the same salient features as $[Ru(bpy)_2(py\text{-}phen)]^{2+}$. $[Ru(py\text{-}phen)_3]^{2+}$ also exhibited single exponential growth kinetics with a significantly faster rate constant, 2.4×10^{11} s^{-1} (4.2 ps). The apparent bleach present at short wavelengths for all delay times results from scattered laser light in the CCD detector and cannot be suppressed. Therefore, no information regarding the dynamics associated with the MLCT chromophore can be acquired in the present experimental apparatus. The instrumental response of this apparatus is 500 fs, and it has been shown that dynamics within MLCT chromophores occurs on shorter time scales.[9,24] Therefore, the growth kinetics associated with the formation of ^{3}pyrene is likely a result of triplet−triplet energy transfer from the ^{3}MLCT excited states.

The steady-state emission spectra of the compounds in the present study measured at 77 K in 4:1 EtOH/MeOH glasses are shown in Figure 6. Ethyl iodide (10%) was added to py-phen to induce phosphorescence. The 77 K spectra of $Ru(bpy)_2(py\text{-}phen)]^{2+}$ and $[Ru(py\text{-}phen)_3]^{2+}$ are superimposable within experimental error (±2 nm) and displayed a peak at 601 nm (16 640 cm^{-1}) with well-defined vibrational structure. The low-temperature luminescence spectra of $[Ru(bpy)_3]^{2+}$ (Figure 6a) exhibits a maximum at 580 nm (17 240 cm^{-1}) with broad features that do not correspond to those seen in either Ru(II)/pyrene complex. The phosphorescence spectrum of py-phen (Figure 6b) has a peak at 598 nm (16 720 cm^{-1}) with vibrational features similar to both Ru(II)/pyrene complexes. The relative intensity of the 77 K phosphorescence bands of py-phen appear to be different than the dyad and tetrad complexes. However, the tail of the singlet fluorescence in py-phen (see Supporting Information) affects these relative intensities, preventing a quantitative comparison.

Low temperature (77 K) time-resolved emission spectra of $[Ru(bpy)_2(py\text{-}phen)]^{2+}$ at 100 ns and 20 μs following a 450 nm laser pulse are shown in Figure 7. The prompt luminescence is dominated by ^{3}MLCT-based emission whereas ^{3}pyrene-like phosphorescence dominates at long delay times. The 77 K data clearly indicate that selective excitation of the MLCT chromophore results in the population of multiple triplet states. It is also interesting to note that the reverse triplet energy transfer processes are no longer favored at 77 K. In the absence of this decay pathway, the pyrene chromophore(s) phosphoresce. The time-resolved emission spectrum of $[Ru(py\text{-}phen)_3]^{2+}$ is similar to that obtained for $[Ru(bpy)_2(py\text{-}phen)]^{2+}$; however, the two distinct emission bands cannot be completely separated in the

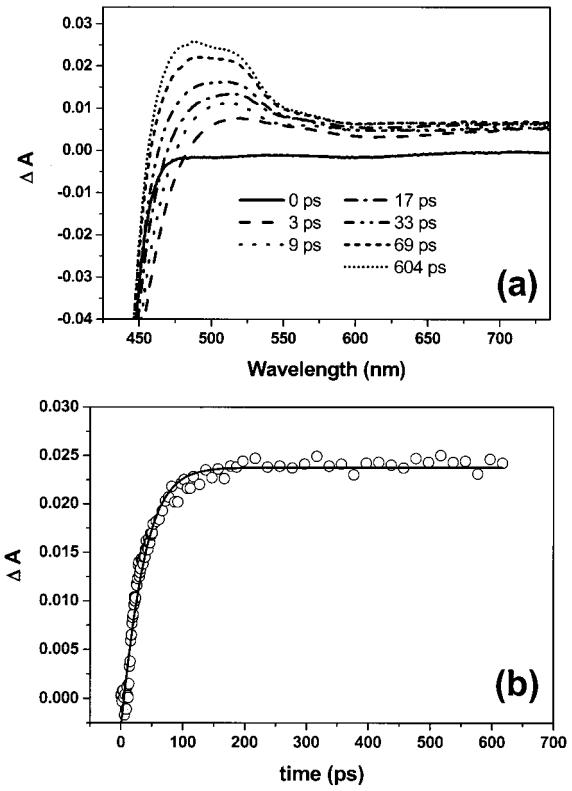

Figure 5. (a) Ultrafast transient differential absorption spectra recorded at various delay times after excitation of $[Ru(bpy)_2(py\text{-}phen)]^{2+}$ with 400 ± 10 nm (150 fs fwhm) pulsed laser excitation. (b) Kinetic profile of the transient at 500 nm (open circles) fit to a single-exponential model (solid line) with a growth rate of 2.8×10^{10} s^{-1} (35.7 ps).

former. This suggests that the ^{3}pyrene state is populated to a larger extent in $[Ru(py\text{-}phen)_3]^{2+}$, which is likely due to the presence of additional pyrenyl units and the wider energy gap between the MLCT and pyrenyl triplet states.

An energy level diagram detailing the photophysical processes in both Ru(II) compounds consistent with our data is given in Figure 8. At room temperature, the ^{1}MLCT state is formed either through direct excitation of the MLCT ground state or via singlet energy transfer from the pyrenyl antenna unit(s). The ^{1}MLCT state undergoes efficient ISC to the ^{3}MLCT state followed by rapid triplet energy transfer forming ^{3}pyrene leading to thermal equilibrium. The triplet state of py-phen is located approximately 600 cm^{-1} below $[Ru(bpy)_3]^{2+}$, facilitating establishment of the equilibrium. The relative partitioning of pyrene (α) and MLCT (1-α) triplets within the equilibrium mixture can be calculated using eq 1,[7,10]

$$K_{eq} = \frac{\alpha}{1-\alpha} = \frac{k_f}{k_r} \qquad (1)$$

where k_f is the rate of triplet energy transfer from the ^{3}MLCT states to the ^{3}pyrene states and k_r is the reverse process. Using a luminescence actinometry experiment similar to that described earlier (see Supporting Information),[7,10] α and K_{eq} can be evaluated independently of any kinetic data. For $[Ru(bpy)_2(py\text{-}phen)]^{2+}$, $\alpha = 0.935$ and $K_{eq} = 14.5$, whereas in $[Ru(py\text{-}phen)_3]^{2+}$, $\alpha = 0.989$ and $K_{eq} = 86.7$. As stated earlier, the rates of formation of triplet pyrene in both complexes were directly measured using ultrafast transient absorption spectroscopy. Combining data from both experiments, the reverse energy transfer rates (k_r) are calculated to be 1.93×10^9 s^{-1} and 2.77×10^9 s^{-1} in the dyad and tetrad, respectively. In both cases,

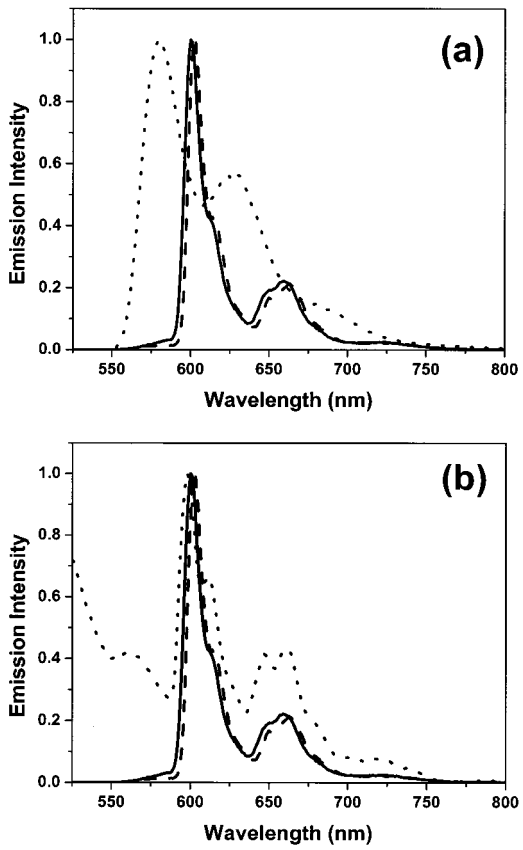

Figure 6. (a) 77 K emission spectra of $[Ru(bpy)_3]^{2+}$ (dotted line), $[Ru(bpy)_2(py\text{-}phen)]^{2+}$ (solid line), and $[Ru(py\text{-}phen)_3]^{2+}$ (dashed line). (b) 77 K emission spectra of py-phen (dotted line), $[Ru(bpy)_2(py\text{-}phen)]^{2+}$ (solid line), and $[Ru(py\text{-}phen)_3]^{2+}$ (dashed line).

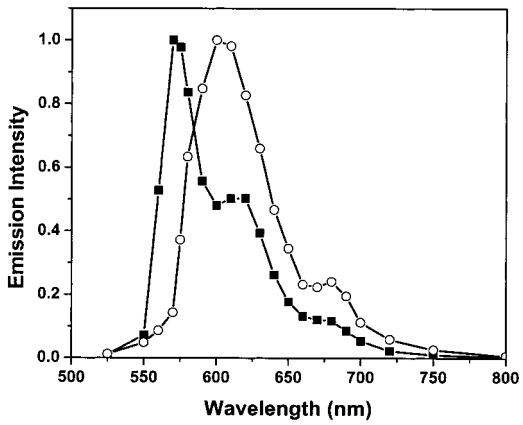

Figure 7. Time-resolved emission spectra of $[Ru(bpy)_2(py\text{-}phen)]^{2+}$ at 100 ns (filled squares) and 20 μs (open circles) after a 458 nm laser pulse measured at 77 K in a 4:1 ethanol/methanol glass.

there are minimal amounts of MLCT excited states present in the equilibrium mixture (6.5 and 1.1%, respectively), permitting the pyrenyl chromophore(s) to dictate the photophysical properties. Consistent with this behavior, there is a large increase in excited-state lifetime in going from $[Ru(bpy)_2(py\text{-}phen)]^{2+}$ (23.7 μs) to $[Ru(py\text{-}phen)_3]^{2+}$ (148 μs).

The long lifetime exhibited by the tetrad (and large K_{eq}) is only partially justified by considering the degeneracy of the pyrene-localized excited states in the dyad (singly degenerate) and tetrad (triply degenerate). The remainder may be explained by taking into account the relative triplet energy levels using slightly different model complexes that more appropriately represent the MLCT energies ($[Ru(bpy)_2(phen)]^{2+}$ and [Ru-

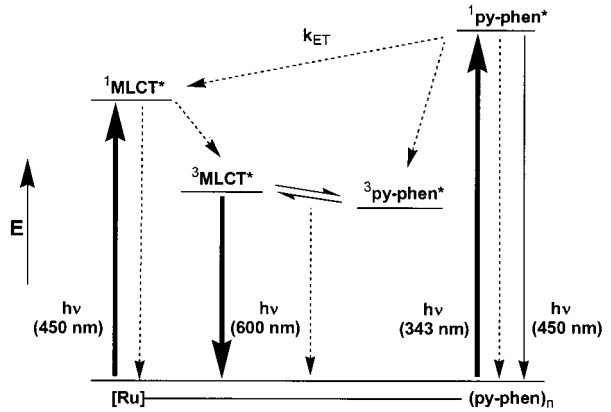

Figure 8. Energy level diagram describing the photophysical processes of $[Ru(bpy)_2(py\text{-}phen)]^{2+}$ and $[Ru(py\text{-}phen)_3]^{2+}$ at room temperature. Solid lines represent radiative transitions and dashed lines represent nonradiative transitions.

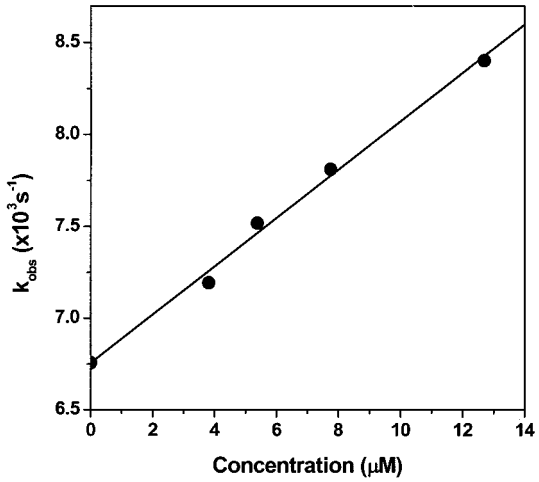

Figure 9. Self-quenching of $[Ru(py\text{-}phen)_3]^{2+}$ measured in deaerated CH_3CN at 22 °C.

$(phen)_3]^{2+}$). The triplet energies of these complexes are 17 420 and 17 670 cm^{-1}, respectively, estimated from their 77 K emission spectra. Using $[Ru(bpy)_2(phen)]^{2+}$ as a model for $[Ru(bpy)_2(py\text{-}phen)]^{2+}$, the energy gap between the MLCT and pyrene triplet states is 780 cm^{-1}. For $[Ru(py\text{-}phen)_3]^{2+}$, this gap increases to 1030 cm^{-1} when $[Ru(phen)_3]^{2+}$ is used as the model. This simple analysis suggests the notably large change in luminescence lifetime can be partially attributed to the differences in the triplet energy gaps in each molecule. Consistent with the model we have previously suggested,[10] the lifetimes (and K_{eq}) observed in the dyad and tetrad are a consequence of degeneracy in the pyrene-localized excited states as well as differences in the ^{3}MLCT-^{3}pyrene energy gap.

Another interesting observation uncovered in this work was the fact that the excited-state lifetime of $[Ru(py\text{-}phen)_3]^{2+}$ was found to be concentration sensitive and could be quantified using a Stern−Volmer quenching analysis (Figure 9).[12] The quenching constant was determined to be 1.3×10^8 M^{-1} s^{-1} measured in concentrations ranging from infinite dilution to 13 μM. There was no evidence for ground-state aggregation in the absorption spectra or exciplex formation in the emission profile over the concentration range employed. At the present time, the nature of the excited-state self-quenching reaction exhibited by $[Ru(py\text{-}phen)_3]^{2+}$ is unclear. However, under the same experimental conditions, $[Ru(bpy)_2(py\text{-}phen)]^{2+}$ displayed a constant, concentration-independent lifetime.

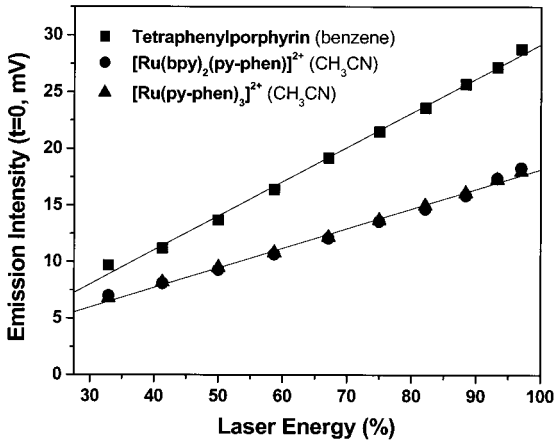

Figure 10. Effect of laser intensity on the initial yield of singlet molecular oxygen for TPP (filled squares), $[Ru(bpy)_2(py\text{-}phen)]^{2+}$ (filled circles), and $[Ru(py\text{-}phen)_3]^{2+}$ (filled triangles) with 532 nm excitation and detected at 1270 nm. Due to solubility, TPP was measured in air-equilibrated C_6H_6 while $[Ru(bpy)_2(py\text{-}phen)]^{2+}$ and $[Ru(py\text{-}phen)_3]^{2+}$ were measured in air-equilibrated CH_3CN. Similar solubilities of molecular oxygen in both solvents (C_6H_6 = 9.06 mM, CH_3CN = 9.1 mM) permitted a quantitative comparison.

A well-documented phenomenon of Ru(II) polypyridine complexes is their ability to sensitize the production singlet oxygen. A quantitative study of the production of singlet oxygen as a function of laser intensity is presented in Figure 10. TPP in deaerated benzene ($\Phi = 0.58$) served as a standard to measure the quantum yields of singlet oxygen generation for $[Ru(bpy)_2(py\text{-}phen)]^{2+}$ and $[Ru(py\text{-}phen)_3]^{2+}$. The signal amplitude, L_0 (mV), due to singlet oxygen emission at $t = 0$, is given by the following expression:[18]

$$L_0 \propto k_r n_\Delta \tag{2}$$

where k_r is the radiative rate constant for the $^1\Delta_g \rightarrow {}^3\Sigma_g^-$ transition of O_2 and n_Δ is the number of O_2 ($^1\Delta_g$) molecules generated upon excitation. The n_Δ component is proportional to the quantum yield of singlet oxygen production (Φ_Δ). The radiative rate constant for the singlet oxygen infrared luminescence is solvent dependent. In general, it is good practice to measure the singlet oxygen standard in the same solvent as the unknown sample.[25] In the present situation, however, no suitable standard in CH_3CN was available and hence a solvent dependence calibration was incorporated into the analysis. The radiative rate constant of singlet oxygen in acetonitrile and benzene solvents has been measured previously, 1.47×10^4 s^{-1} ($\tau = 68$ μs) and 3.13×10^4 s^{-1} ($\tau = 32$ μs), respectively.[19,26] The parameter n_Δ depends on the ground-state absorbance of the sample at the excitation wavelength and the energy of the excitation light. Singlet oxygen is produced in a bimolecular process, and therefore n_Δ is dependent on the fraction of donor excited states quenched by O_2. The quenching efficiencies (η) can be calculated from eq 3:[18]

$$\eta = \frac{k_q[O_2]}{(\tau_0^{-1} + k_q[O_2])} \tag{3}$$

where τ_0 is the lifetime of the excited state of the donor. For TPP and ruthenium(II) polypyridine complexes, typical values for k_q are on the order of 10^9 s^{-1}.[18] For donors with lifetimes greater than a few microseconds, the excited states are sufficiently long-lived that all are quenched by molecular oxygen and the assumption that $\eta = 1$ can be made. The concentration

of dissolved oxygen in room-temperature air equilibrated solutions of benzene and acetonitrile is the same, (C_6H_6 = 9.06 mM, CH_3CN = 9.1 mM).[27] Therefore,

$$L_0 \propto B\Phi_\Delta k_r \eta AE \tag{4}$$

where B is an instrument factor, A is the ground state absorbance at the excitation wavelength, and E is the energy of the excitation pulse. At low laser pulse energies, typically ~10 mJ, L_0 changes linearly with laser energy for both the reference standard and the samples, Figure 10. The slopes for reference (r) and unknown (x) were calculated and used to determine the quantum yield of singlet oxygen formation for the unknown, Φ_Δ^x, as follows:

$$\Phi_\Delta^x = \frac{(\text{slope}^x)\Phi_\Delta^r k_r^r}{(\text{slope}^r)k_r^x} \tag{5}$$

The plots for $[Ru(bpy)_2(py\text{-}phen)]^{2+}$ and $[Ru(py\text{-}phen)_3]^{2+}$ are superimposable, yielding the same value for singlet oxygen quantum yield in acetonitrile, $\Phi_\Delta = 0.69$. Due to the relatively short lifetimes of the complexes compared with tetraphenylporphyrin in benzene, this value must be considered an estimate for the lower limit of the singlet oxygen quantum yield. The singlet oxygen quantum yields for the quenching of $[Ru(bpy)_3]^{2+}$ and analogous $[Ru(bpy)_{3-z}]^{2+}$ complexes containing z = 0, 1, 2, 3 bipyrimidine and bipyrazine ligands by molecular oxygen have been determined previously.[28] In general, all of these complexes had quantum yields of unity for singlet oxygen production with the notable exception of $[Ru(bpy)_3]^{2+}$, which had $\Phi_\Delta = 0.5 \pm 0.4$.[18,28] The lower value for $[Ru(bpy)_3]^{2+}$ is a result of a competitive electron-transfer process.[18] However, in the present work, the excited states of $[Ru(bpy)_2(py\text{-}phen)]^{2+}$ and $[Ru(py\text{-}phen)_3]^{2+}$ are dominated by pyrene triplet states and not the MLCT excited state. The quantum yield for singlet oxygen formation from pyrene in both toluene and cyclohexane is unity.[29,30] A quantum yield of 0.69 for the production of singlet O_2 in $[Ru(bpy)_2(py\text{-}phen)]^{2+}$ and $[Ru(py\text{-}phen)_3]^{2+}$ in CH_3CN indicates that other deactivation pathways may be competitive with singlet oxygen sensitization.

Conclusion

The present work utilizes pyrene chormophores to produce Ru(II)-based UV light-harvesting complexes that possess extended excited-state lifetimes. These lifetimes are obtained without relying on energy gap law predictions. Upon UV irradiation, the pyrene units serve as an antenna system that gathers and funnels photonic energy to the Ru(II) core. In both complexes, the pyrene antenna then switches from energy donor to energy acceptor as the excited-state triplet equilibrium becomes established. The substantial increase in the excited-state lifetime in going from $[Ru(bpy)_2(py\text{-}phen)]^{2+}$ to $[Ru(py\text{-}phen)_3]^{2+}$ is a combined result of increasing the number of pyrenyl units and a larger triplet energy gap in the latter, substantially favoring "pyrene-like" triplets in the equilibrium mixture. The long lifetime associated with $[Ru(py\text{-}phen)_3]^{2+}$ permits a dynamic excited state self-quenching reaction at room temperature, the origin of which remains under investigation. Both Ru(II) complexes were also found to sensitize the production of singlet oxygen with relatively high efficiency. The incorporation of selected organic chromophores into MLCT structures can markedly enhance the photophysical properties exhibited by the latter, important for potential applications in emerging luminescence-based technologies.

Acknowledgment. D.S.T. was supported through a Hammond Fellowship of the McMaster Endowment administered by the Center for Photochemical Sciences at BGSU. J.B. was supported through the National Science Foundation Research Experience for Undergraduates program.

Supporting Information Available: Fluorescence spectra of pyrene and py-phen are provided along with the data used in the luminescence actinometry experiments. This material is available free of charge via the Internet at http://pubs.acs.org.

References and Notes

(1) Lakowicz, J. R. *Principles of Fluorescence Spectroscopy*; Kluwer Academic/Plenum Publishers: New York, 1999.

(2) Terptschnig, E.; Szmacinski, H.; Malak, H.; Lakowicz, J. R. *Biophys. J.* **1995**, *68*, 342.

(3) Guo, X.-Q.; Castellano, F. N.; Li, L.; Lakowicz, J. R. *Anal. Chem.* **1998**, *70*, 632.

(4) (a) *Topics in Fluorescence Spectroscopy Vol. 4: Probe Design and Chemical Sensing*; Lakowicz, J. R., Ed.; Plenum Press: New York, 1994. (b) Lakowicz, J. R.; Castellano, F. N.; Dattelbaum, J. D.; Tolosa, L.; Rao, G.; Gryczynski, I. *Anal. Chem.* **1998**, *70*, 5115.

(5) For a review see: Juris, A.; Balzani, V.; Barigelletti, F.; Campagna, S.; Belser, P.; von Zelewsky, A. *Coord. Chem. Rev.* **1988**, *84*, 85.

(6) Ford, W. E.; Rodgers, M. A. J. *J. Phys. Chem.* **1992**, *96*, 2917.

(7) (a) Wilson, G. J.; A.; Sasse, W. H. F.; Mau, A. W. H *Chem. Phys. Lett.* **1996**, *250*, 583. (b) Wilson, G. J.; Launikonis, A.; Sasse, W. H. F.; Mau, A. W. H. *J. Phys. Chem. A* **1997**, *101*, 4860. (c) Wilson, G. J.; Launikonis, A.; Sasse, W. H. F.; Mau, A. W. H. *J. Phys. Chem. A* **1998**, *102*, 5150.

(8) Harriman, A.; Hissler, M.; Khatyr, A.; Ziessel, R. *Chem. Commun.* **1999**, 735.

(9) Hissler, M.; Harriman, A.; Khatyr, A.; Ziessel, R. *Chem. Eur. J.* **1999**, *5*, 3366.

(10) Tyson, D. S.; Castellano, F. N. *J. Phys. Chem. A* **1999**, *103*, 10955.

(11) Simon, J. A.; Curry, S. L.; Schemhl, R. H.; Schatz, T. R.; Piotrowiak, P.; Jin, X.; Thummel, R. P. *J. Am. Chem. Soc.* **1997**, *119*, 11012.

(12) Tyson, D. S.; Bialecki, J.; Castellano, F. N. *Chem. Commun.* **2000**, 2355.

(13) Sullivan, B. P.; Salmon, D. J.; Meyer, T. J. *Inorg. Chem.* **1978**, *17*, 3334.

(14) Evans, I. P.; Spencer, A.; Wilkinson, G. *J. Chem. Soc., Dalton Trans.* **1973**, 204.

(15) Hissler, M.; Connick, W. B.; Geiger, D. K.; McGarrah, J. E.; Lipa, D.; Lachicotte, R. J.; Eisenberg, R. *Inorg. Chem.* **2000**, *39*, 447.

(16) Gumprecht, W. H. *Org. Synth.* **1968**, *48*, 30.

(17) Nikoloaitchick, A. V.; Korth, O.; Rodgers, M. A. J. *J. Phys. Chem. A* **1999**, *103*, 7587.

(18) Zhang, X.; Rodgers, M. A. J. *J. Phys. Chem.* **1995**, *99*, 12797.

(19) Gorman, A. A.; Rodgers, M. A. J., Singlet Oxygen, Chapter 10 in *Handbook of Organic Photochemistry Volume II*, Scaiano, J. C., Ed., CRC Press: Boca Raton, 1987.

(20) Halgren, T. A. *J. Comput. Chem.* **1996**, *17*, 490.

(21) Soujanya, T.; Philippon, A.; Leroy, S.; Vallier, M.; Fages, F. *J. Phys. Chem. A* **2000**, *104*, 9408.

(22) Both complexes could be fit to a single exponential model on time scales adequate to capture the entire decay on the oscilloscope. When the early time regions are expanded, the dyad complex clearly contains a minor short component ~1 μs. See text for details.

(23) Baba, A. I.; Shaw, J. R.; Simon, J. A.; Thummel, R. P.; Schemehl, R. H. *Coord. Chem. Rev.* **1998**, *171*, 43.

(24) (a) Damrauer, N. H.; Cerullo, G.; Yeh, A. T.; Boussie, T. R.; Shank, C. V.; McCusker, J. K. *Science* **1997**, *275*, 54. (b) Yeh, A. T.; Shank, C. V.; McCusker, J. K. *Science* **2000**, *289*, 935.

(25) Gorman, A. A.; Krasnovsky, A. A.; Rodgers, M. A. J.; *J. Phys. Chem.* **1991**, *95*, 598.

(26) Hurst, J. R.; McDonald J. D.; Schuster, G. B.; *J. Am. Chem. Soc.* **1982**, *104*, 2065.

(27) Murov, S. L.; Carmichael, I.; Hug, G. L. *Handbook of Photochemistry*, 2nd ed.; Marcel Decker: New York, 1993.

(28) Mulazzani Q. G.; Sun, H.; Hoffman, M. Z.; Ford, W. E.; Rogers M. A. J. *J. Phys. Chem.* **1994**, *98*, 1145.

(29) Gurinovich, G. P.; Salokhiddinov, K. L. *Chem. Phys. Lett.* **1982**, *85*, 9.

(30) Usui, Y.; Shimizu, N.; Mori S. *Bull. Chem. Soc. Jpn.* **1992**, *65*, 897.